
Phase diagram of the three-band d-p model based on the optimization variational Monte Carlo method

^aTAKASHI YANAGISAWA, ^bMITAKE MIYAZAKI, ^aKUNIHICO YAMAJI

^a*Electronics and Photonics Research Institute, National Institute of Advanced Industrial Science and Technology (AIST), Tsukuba Central 2, 1-1-1 Umezono, Tsukuba 305-8568, Japan*

^b*Hakodate Institute of Technology, 14-1 Tokura, Hakodate, Hokkaido 042-8501, Japan*

PACS 71.10.-w – First pacs description
PACS 71.27.+a – Second pacs description
PACS 71.10.Fd – Third pacs description

Abstract – The phase diagram of cuprate high-temperature superconductors is investigated on the basis of the three-band d-p model. We use the optimization variational Monte Carlo method, where improved many-body wave functions have been proposed to make the ground-state wave function more precise. We investigate the stability of antiferromagnetic state by changing the band parameters such as the hole number, level difference Δ_{dp} between d and p electrons and transfer integrals. We show that the antiferromagnetic correlation weakens when Δ_{dp} decreases and the pure d -wave superconducting phase may exist in this region. We present phase diagrams including antiferromagnetic and superconducting regions by varying the band parameters. The phase diagram obtained by changing the doping rate x contains antiferromagnetic, superconducting and also phase-separated phases. We propose that high-temperature superconductivity will occur near the antiferromagnetic boundary in the space of band parameters.

Introduction. – The physics of high-temperature superconductivity has been studied from the viewpoint of strongly correlated electron systems since its discovery [1]. This is because cuprate parent materials are Mott insulators and the Cooper pairs have the d-wave symmetry. The fundamental model of cuprate high-temperature superconductors is the electronic model for the CuO_2 plane including copper and oxygen atoms. This model is called the d-p model (or three-band Hubbard model) [2–18]. It is certain that the electron correlation plays an important role in the d-p model since the on-site Coulomb interaction U_d between d electrons is large. This makes it a difficult task to understand the phase diagram of the d-p model. Because U_d is the large-energy scale interaction, new phenomena including high-temperature superconductivity can be expected. Simplified models such as the two-dimensional single-band Hubbard model [19–40] or ladder model [41–46] have been studied to investigate whether the attractive interaction is induced from the on-site Coulomb interaction.

We employ the optimization variational Monte Carlo method to investigate electronic properties of the three-band d-p model. In this method we calculate the expecta-

tion values of several physical properties numerically using a Monte Carlo algorithm [47–49]. In order to control the strong electron correlation, we use the Gutzwiller function and wave functions that are improved by multiplying an initial wave function by $\exp(-K)$ -type operators [36, 49], where K is a correlation operator with variational parameters. In this paper, K stands for the non-interacting part of the Hamiltonian. In the single-band Hubbard model, the ground-state energy is lowered greatly and becomes lower than that obtained by other wave functions [36].

The single-band Hubbard model is the fundamental model and was used to understand the metal-insulator transition [50] and magnetic properties [51]. It has been shown from numerical studies based on improved wave functions that the superconducting phase exists in the single-band two-dimensional (2D) Hubbard model [31, 36, 37, 52, 53]. We regard the multi-band model as a more realistic model of high-temperature superconductors.

In this paper we investigate the stability of antiferromagnetically ordered state in the two-dimensional d-p model. The phase diagram is determined as a result of the competition between antiferromagnetic (AF) and superconducting (SC) pair correlations. The AF region de-

creases as the level difference $\epsilon_p - \epsilon_d$ decreases and thus the pure d-wave pairing phase may exist when $\epsilon_p - \epsilon_d$ is small. There is a phase separation (PS) in the low-doping region as in the two-dimensional Hubbard model [54–58]. We show the phase diagram as a function of the doping rate to show AF, SC and PS regions in the d-p model. We think that high-temperature superconductivity occurs in the crossover region near the boundary of AF phase [36, 37]. In the single-band Hubbard model, the crossover takes place as the on-site Coulomb interaction U increases (or decreases). In the three-band d-p model, there are several parameters that can control AF correlation and would induce crossovers where AF or charge fluctuations grow larger.

Hamiltonian. – We consider the three-band d-p model in this paper. The Hamiltonian is written as

$$\begin{aligned}
 H = & \epsilon_d \sum_{i\sigma} d_{i\sigma}^\dagger d_{i\sigma} + \epsilon_p \sum_{i\sigma} (p_{i+\hat{x}/2\sigma}^\dagger p_{i+\hat{x}/2\sigma} \\
 & + p_{i+\hat{y}/2\sigma}^\dagger p_{i+\hat{y}/2\sigma}) \\
 & + t_{dp} \sum_{i\sigma} [d_{i\sigma}^\dagger (p_{i+\hat{x}/2\sigma} + p_{i+\hat{y}/2\sigma} - p_{i-\hat{x}/2\sigma} - p_{i-\hat{y}/2\sigma}) \\
 & + \text{h.c.}] \\
 & + t_{pp} \sum_{i\sigma} [p_{i+\hat{y}/2\sigma}^\dagger p_{i+\hat{x}/2\sigma} - p_{i+\hat{y}/2\sigma}^\dagger p_{i-\hat{x}/2\sigma} \\
 & - p_{i-\hat{y}/2\sigma}^\dagger p_{i+\hat{x}/2\sigma} + p_{i-\hat{y}/2\sigma}^\dagger p_{i-\hat{x}/2\sigma} + \text{h.c.}] \\
 & + t'_d \sum_{\langle\langle ij \rangle\rangle\sigma} (d_{i\sigma}^\dagger d_{j\sigma} + \text{h.c.}) + U_d \sum_i d_{i\uparrow}^\dagger d_{i\uparrow} d_{i\downarrow}^\dagger d_{i\downarrow}. \quad (1)
 \end{aligned}$$

$d_{i\sigma}$ and $d_{i\sigma}^\dagger$ represent the operators for the d hole, and $p_{i\pm\hat{x}/2\sigma}$ and $p_{i\pm\hat{y}/2\sigma}^\dagger$ denote the operators for the p holes at the site $R_{i\pm\hat{x}/2}$, and in a similar way $p_{i\pm\hat{y}/2\sigma}$ and $p_{i\pm\hat{x}/2\sigma}^\dagger$ are defined. t_{dp} and t_{pp} represent the transfer integrals between adjacent Cu and O orbitals and that between nearest neighbor p orbitals, respectively. t'_d was introduced to reproduce the Fermi surface [59] for cuprate superconductors. U_d denotes the on-site Coulomb repulsion and U_p is that between p holes. In general, U_p is smaller than U_d [60–64].

The values of band parameters have been estimated in the literature. For example, $U_d = 10.5$, $U_p = 4.0$ and $U_{dp} = 1.2$ in eV [61] where U_{dp} is the nearest-neighbor Coulomb interaction between holes on adjacent Cu and O orbitals. We neglect U_{dp} because U_{dp} is small compared to U_d . The level difference between d and p holes is denoted as $\Delta_{dp} = \epsilon_p - \epsilon_d$. N stands for the number of sites and the total number of atoms is given by $N_a = 3N$. The energy measured in units of t_{dp} in this paper. We use the hole picture and we consider the case where $\Delta_{dp} \geq 0$ in this paper.

Improved wave functions with electron correlation. – The wave function is given as

$$\psi_\lambda = \exp(-\lambda K) \psi_G, \quad (2)$$

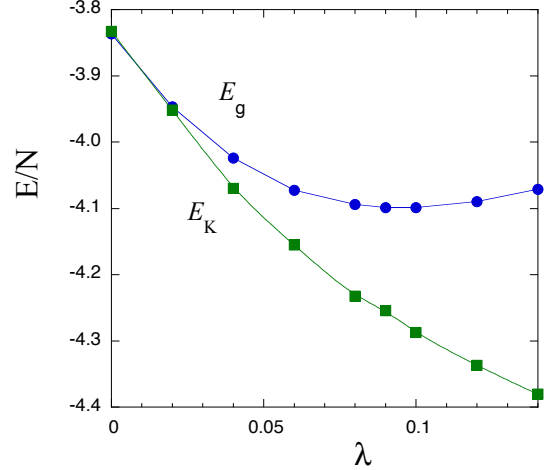


Fig. 1: Ground-state energy E_g and the kinetic energy $E_K = \langle K \rangle$ as a function of λ on an 8×8 lattice with 76 holes. The band parameters are $\epsilon_p - \epsilon_d = 2t_{dp}$, $t_{pp} = 0.4$, $t'_d = -0.2$, $U_d = 10$ and $U_p = 0$ where the energy unit is t_{dp} .

where K denotes the non-interacting part of the Hamiltonian: $K = H$ with $U_d = 0$. λ is a real variational parameter. ψ_G is given as $\psi_G = P_G \psi_0$, with $P_G = \prod_i [1 - (1-g)n_{d_i\uparrow}n_{d_i\downarrow}]$ where g takes the value in the range $0 \leq g \leq 1$. This is the wave function which is improved from the Gutzwiller function [36, 37, 49, 53, 65–69] generalized to the three-band model [70] by multiplying by an exponential factor. ψ_0 is a one-particle state with variational parameters \tilde{t}_{dp} , \tilde{t}_{pp} , \tilde{t}'_d , $\tilde{\epsilon}_p - \tilde{\epsilon}_d$ [70]: $\psi_0 = \psi_0(\tilde{t}_{dp}, \tilde{t}_{pp}, \tilde{t}'_d, \tilde{\epsilon}_p - \tilde{\epsilon}_d)$. ψ_0 is obtained as the eigenstate of the non-interacting Hamiltonian with these variational parameters. We set $\tilde{t}_{dp} = t_{dp}$ and the energy is measured in units of t_{dp} . K also contains variational parameters: $K = K(\tilde{t}_{pp}, \tilde{t}'_d, \tilde{\epsilon}_p - \tilde{\epsilon}_d)$. The expectation values are calculated by using the variational Monte Carlo method.

We here give a discussion on the role K in the wave function. The operator $e^{-\lambda K}$ controls the weights of excitation modes in the Gutzwiller function. $e^{-\lambda K}$ suppresses high-energy excitations for which the eigenvalues of K are large and thus $e^{-\lambda k}$ becomes small. This indicates that $e^{-\lambda K}$ plays a role of projection that projects out low lying excitation modes from the wave function. This appears in the behavior of the momentum distribution function $n_{\mathbf{k}\sigma} \equiv \langle c_{\mathbf{k}\sigma}^\dagger c_{\mathbf{k}\sigma} \rangle$. In fact, $n_{\mathbf{k}\sigma}$ evaluated by the Gutzwiller function shows an unphysical behavior, that is, $n_{\mathbf{k}\sigma}$ at \mathbf{k} near the Fermi surface is often larger than that at the bottom of the band [71]. This shortcoming is remedied by the improved wave function [59].

We show the energy-expectation value as a function of λ in Fig. 1 where calculations were performed on the system of 8×8 lattice with 76 holes. E_K denotes the expectation value $E_K = \langle K \rangle$. The parameters are $\Delta_{dp} = \epsilon_p - \epsilon_d = 2$, $t_{pp} = 0.4$, $t'_d = -0.2$ and $U_d = 10$ in units of t_{dp} . The lowering of the total energy originates from the kinetic-energy gain as λ is increased. The total energy given by

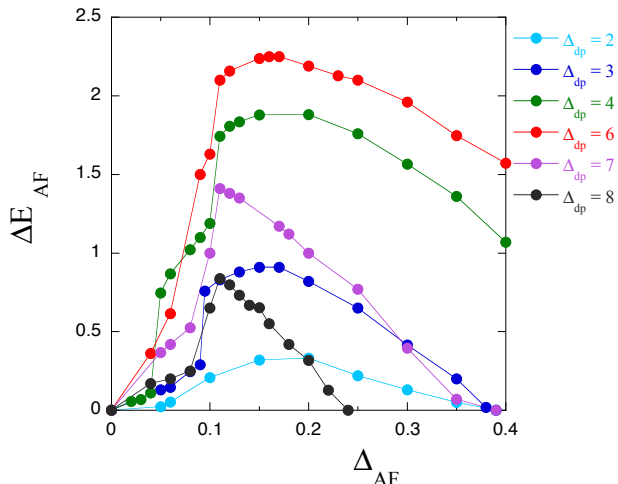


Fig. 2: Antiferromagnetic condensation energy for ψ_λ as a function of the AF gap parameter Δ_{AF} for several values of the level difference $\Delta_{dp} \equiv \epsilon_p - \epsilon_d$. We carried out calculations on an 8×8 lattice (192 atoms) with 76 holes (where the doping rate x is $x = 0.1875$). We set $t_{pp} = 0.4$, $t'_d = 0$ and $U_d = 10$ in units of t_{dp} .

the sum of the kinetic energy and the potential energy has a minimum at finite value of λ . Since the Coulomb potential energy increases as λ increases, the total energy is determined by the balance between the kinetic energy and the Coulomb energy.

The correlated BCS wave function is written as

$$\psi_{\lambda-BCS} = \exp(-\lambda K) P_G \prod_{\mathbf{k}} (u_{\mathbf{k}} \beta_{\mathbf{k}}^\dagger + v_{\mathbf{k}} \alpha_{\mathbf{k}}^\dagger) |\tilde{0}\rangle, \quad (3)$$

where the particle-hole transformation for down-spin holes [36, 53] has been performed: $\beta_{\mathbf{k}}^\dagger = \alpha_{-\mathbf{k}\downarrow}$ and $\alpha_{\mathbf{k}}^\dagger = \alpha_{\mathbf{k}\uparrow}$. $|\tilde{0}\rangle$ denotes the vacuum for newly defined α and β particles satisfying $\alpha_{\mathbf{k}}|\tilde{0}\rangle = \beta_{\mathbf{k}}|\tilde{0}\rangle = 0$. The BCS parameter is given by the conventional form $v_{\mathbf{k}}/u_{\mathbf{k}} = \Delta_{\mathbf{k}}/(\xi_{\mathbf{k}} + \sqrt{\xi_{\mathbf{k}}^2 + \Delta_{\mathbf{k}}^2})$, where $\xi_{\mathbf{k}}$ is the dispersion relation of the lowest band we assume the d-wave symmetry $\Delta_{\mathbf{k}} = \Delta(\cos k_x - \cos k_y)$. $\Delta = \Delta_{sc}$ is a variational parameter and the optimized value Δ_{sc} is regarded as the superconducting gap. In this representation, the electron pair operator $\alpha_{\mathbf{k}\uparrow}^\dagger \alpha_{\mathbf{k}\downarrow}^\dagger$ is transformed to the hybridization form $\alpha_{\mathbf{k}}^\dagger \beta_{\mathbf{k}}$. The chemical potential is used to adjust the expectation value of the total electron number.

Antiferromagnetic state and the level difference.

– The antiferromagnetic wave function is formulated by introducing the AF order parameter Δ_{AF} in the initial wave function $\psi_0(\Delta_{AF})$:

$$\psi_\lambda = \exp(-\lambda K) P_G \psi_0(\Delta_{AF}). \quad (4)$$

The level difference $\Delta_{dp} = \epsilon_p - \epsilon_d$ plays an important role in determining the stability of the AF state. We show the AF condensation energy ΔE_{AF} as a function of the AF

order parameter Δ_{AF} for several values of the level difference between d and p electrons in Fig. 2. We carried out calculations on a system of 8×8 lattice with 192 atoms including copper and oxygen atoms. ΔE_{AF} has a maximum when the level difference Δ_{dp} is about half of U_d , namely, near the 'symmetric case' with $\Delta_{dp} = U_d/2$. In Fig. 2, we set the parameters as $t_{pp} = 0.4$, $t'_d = 0$ and $U_d = 10$ in units of t_{dp} , and the doping rate is $x = 0.1875$. We show $\Delta E_{AF}/N$ as a function of the level difference Δ_{dp} for $t'_d = 0$ and -0.2 in Fig. 3. The AF order parameter Δ_{AF} at which ΔE_{AF} takes a maximum value is shown in Fig. 4 for each value of Δ_{dp} . For $t'_d = 0$, Δ_{AF} vanishes when $\Delta_{dp} \simeq 1$. This indicates that we may have a superconducting phase when the d-hole level is near the p-hole level. The results in Figs. 3 and 4 also show that t'_d suppresses the magnetic instability.

We show $\Delta E_{AF}/N$ as a function of Δ_{dp} when the doping rate is $x = 0.125$ in Fig. 5. The Fig. 5 shows that ΔE_{AF} has also a maximum for $\Delta_{dp} \sim U_d/2$ and AF correlation survives even up to the region of small $\Delta_{dp} \sim 1$ for small x .

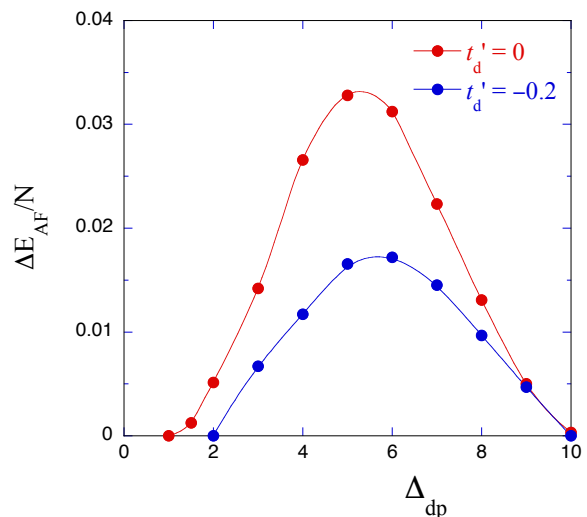


Fig. 3: Antiferromagnetic condensation energy for ψ_λ as function of the level difference $\Delta_{dp} = \epsilon_p - \epsilon_d$ on an 8×8 lattice with 76 holes. We used $t_{pp} = 0.4$ and $U_d = 10$ in units of t_{dp} .

Superconducting state. – First we examine the superconducting state by employing the BCS-Gutzwiller wave function $\psi_{G-BCS} = P_{N_e} P_G \psi_{BCS}$, where ψ_{BCS} indicates the BCS wave function. P_{N_e} is the number-projection operator that extracts only the states with a fixed total hole number. We show the SC condensation energy as a function of the SC order parameter Δ_{sc} in Fig. 6 for several values of the level difference Δ_{dp} . The result shows that the SC condensation energy increases as Δ_{dp} increases. Based on the BCS-Gutzwiller function, the large level difference is more favorable for superconductivity. We should, however, remember instability toward antiferromagnetic state when the level difference Δ_{dp}

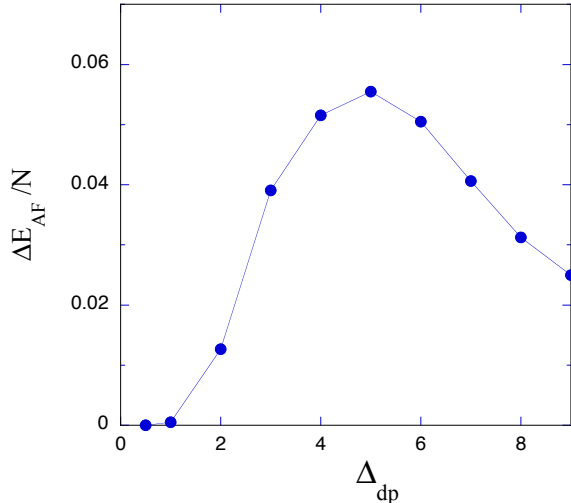


Fig. 4: Antiferromagnetic condensation energy for ψ_λ as function of the level difference Δ_{dp} on an 8×8 lattice with 72 holes ($x = 0.125$). We set $t_{pp} = 0.4$, $t'_d = 0$ and $U_d = 10$.

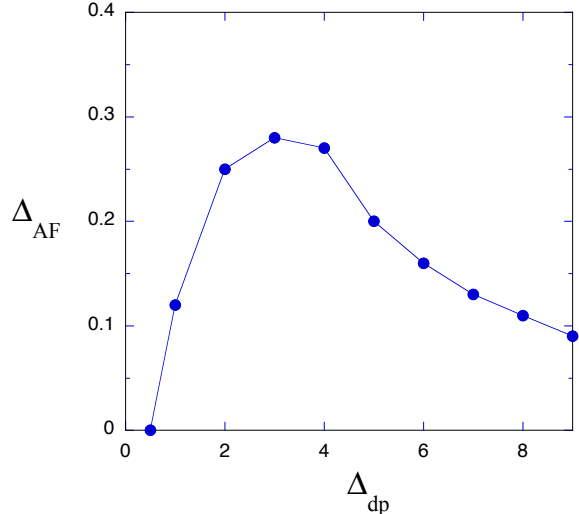


Fig. 5: Antiferromagnetic order parameter for ψ_λ as function of the level difference Δ_{dp} on an 8×8 lattice with 72 holes. The parameters are the same as in Fig.5.

becomes large.

From the competition between AF and SC orderings, we expect that the pure d -wave SC state is stabilized when $\epsilon_d - \epsilon_p$ is near the boundary of the AF region. The AF and SC order parameters are shown as a function of Δ_{dp} in Fig. 7 for $x = 0.1875$. We included the SC order parameter for the Gutzwiller function for reference when $\Delta_{dp} \geq 2t_{dp}$ although SC state is no longer stable in this region. This figure indicates that the SC state exists when the level difference is small and that high-temperature superconductivity will occur in the small Δ_{dp} -region.

Phase diagram and phase separation. – Let us examine the possible phase diagram of cuprate superconductors based on the optimization variational Monte Carlo method. We exhibit the condensation energy as a function of the doping rate x for $\Delta_{dp} = t_{dp}$ in Fig. 8. There is the AF region when x is small and the SC region exists near the optimum region $x \sim 0.2$. We should mention that there is a phase-separated region in the low-doping region where $x < 0.07$. This indicates the existence of AF insulator phase in the low doping region. This is similar to the phase diagram of the 2D Hubbard model. The phase separation (PS) is, however, dependent on the level difference Δ_{dp} . As Δ_{dp} decreases, the phase-separated region decreases and vanishes when Δ_{dp} approaches zero. Thus the area of phase-separated region can be controlled by changing the band parameters.

We lastly show the phase diagram in the U_d - Δ_{dp} plane for $x = 0.1875$ with $t_{pp} = 0.4t_{dp}$ and $t'_d = 0$ in Fig. 9. There are a large AF region and paramagnetic (PM) phase in Fig. 9 where SC regions are not explicitly included. We expect that high-temperature superconductivity may be realized in the relatively small region near the boundary between AF and PM regions.

Summary. – We have investigated the ground-state properties of the three-band d-p model on the basis of the optimization variational Monte Carlo method. The ground-state energy is lowered greatly by multiplying by the exponential operator $e^{-\lambda K}$ as in the 2D Hubbard model. In general, the antiferromagnetic correlation is suppressed as the wave function is improved.

In the d-p model the AF correlation is very much stronger than that in the single-band Hubbard model. It is thus important to control the strength of AF correlation by varying the interaction and band parameters. The level difference Δ_{dp} plays an important role in the study of the phase diagram of the d-p model. The pure d -wave superconducting phase exists when Δ_{dp} becomes small. In particular high-temperature superconductivity is expected near the AF boundary in the small Δ_{dp} region.

A phase-separated region exists in the d-p model as in the single-band 2D Hubbard model. In this region the ground state is an insulator with AF order and is dependent upon Δ_{dp} . The PS region increases as Δ_{dp} increases and decreases and vice versa. The close relation between PS region and incommensurate phases have been examined [56, 57]. The PS instability may be related to an instability toward some charge order such as stripes.

The phase diagram in Fig. 9 is consistent with several experiments concerning the critical temperature T_c of cuprate superconductors [72, 73]. There is a correlation between T_c and the ratio of hole numbers n_p/n_d where n_p and n_d denote the hole density of p and d holes, respectively [72]. There is the tendency that T_c is higher for larger n_p/n_d , that is, T_c increases with the decrease of $\epsilon_p - \epsilon_d$. This is consistent with our result that the pure d -wave pairing state exists when $\epsilon_p - \epsilon_d$ is small.

The increase of T_c under pressure [73] is understood

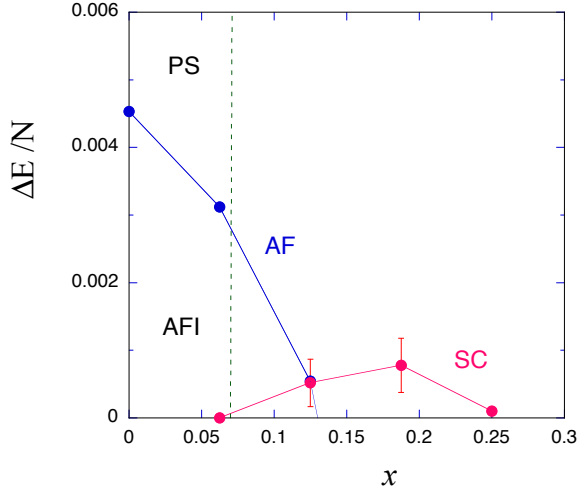


Fig. 8: AF and SC condensation energies as a function of the hole doping rate x for $\Delta_{dp} = 1$ on a 8×8 lattice with $t_{pp} = 0.4$, $t'_d = 0$ and $U_d = 10$ in units of t_{dp} . There is a phase-separated region when x is small.

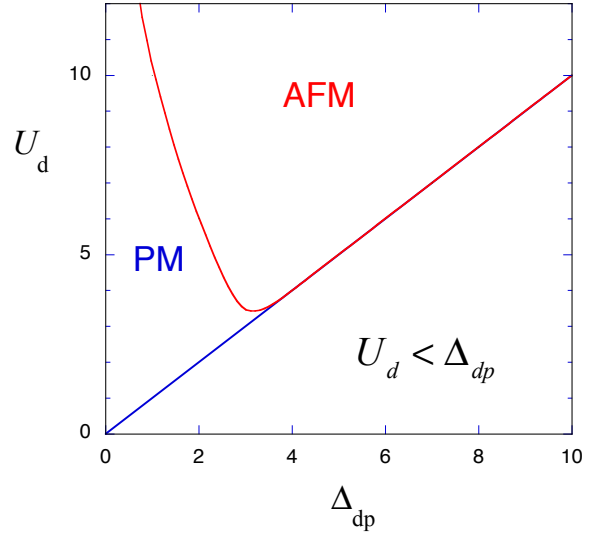


Fig. 9: AF region in the plane of U_d and the level difference Δ_{dp} for $x = 0.1875$ on an 8×8 lattice. We set $t_{pp} = 0.4$ and $t'_d = 0$, and the energy is measured in units of t_{dp} .

- [22] S. Zhang, J. Carlson and J. E. Gubernatis, Phys. Rev. B **55**, 7464 (1997).
- [23] S. Zhang, J. Carlson and J. E. Gubernatis, Phys. Rev. Lett. **78**, 4486 (1997).
- [24] Yanagisawa T and Shimoi Y 1996 *Int. J. Mod. Phys. B* **10** 3383.
- [25] T. Nakanishi, K. Yamaji and T. Yanagisawa, J. Phys. Soc. Jpn. **66**, 294 (1997).
- [26] K. Yamaji, T. Yanagisawa, T. Nakanishi and S. Koike, Physica C **304**, 225 (1998).
- [27] K. Yamaji, T. Yanagisawa, M. Miyazaki and R. Kadono, J. Phys. Soc. Jpn. **80**, 083702 (2011).
- [28] T. M. Hardy, P. Hague, J. H. Samson and A. S. Alexandrov, Phys. Rev. B **79**, 212501 (2009).
- [29] N. Bulut, Adv. Phys. **51**, 1587 (2002).
- [30] H. Yokoyama, Y. Tanaka, M. Ogata and H. Tsuchiura, J. Phys. Soc. Jpn. **73**, 1119 (2004).
- [31] H. Yokoyama, M. Ogata and Y. Tanaka, J. Phys. Soc. Jpn. **75**, 114706 (2006).
- [32] T. Aimi and M. Imada, J. Phys. Soc. Jpn. **76**, 113708 (2007).
- [33] M. Miyazaki, T. Yanagisawa and K. Yamaji, J. Phys. Soc. Jpn. **73**, 1643 (2004).
- [34] T. Yanagisawa, New J. Phys. **10**, 023014 (2008).
- [35] T. Yanagisawa, New J. Phys. **15**, 033012 (2013).
- [36] T. Yanagisawa, J. Phys. Soc. Jpn. **85**, 114707 (2016).
- [37] T. Yanagisawa, J. Phys. Soc. Jpn. **88**, 054702 (2019).
- [38] T. Yanagisawa, Condensed Matter **4**, 57 (2019).
- [39] T. Yanagisawa, Phys. Lett. A **403**, 127382 (2021).
- [40] T. Yanagisawa, Condensed Matter **6**, 12 (2021).
- [41] R. M. Noack, S. R. White and D. J. Scalapino, EPL **30**, 163 (1995).
- [42] R. M. Noack, N. Bulut, D. J. Scalapino and M. G. Zacher, Phys. Rev. B **56**, 7162 (1997).
- [43] K. Yamaji, Y. Shimoi and T. Yanagisawa, Physica C **235**, 2221 (1994).
- [44] S. Koike, K. Yamaji, and T. Yanagisawa, J. Phys. Soc. Jpn. **68**, 1657 (1999).
- [45] T. Yanagisawa, Y. Shimoi and K. Yamaji, Phys. Rev. B **52**, R3860 (1995).
- [46] T. Nakano, K. Kuroki and S. Onari, Phys. Rev. B **76**, 014515 (2007).
- [47] R. Blankenbecler, D. J. Scalapino and R. L. Sugar, Phys. Rev. D **24**, 2278 (1981).
- [48] T. Yanagisawa, Phys. Rev. B **75**, 224503 (2007).
- [49] T. Yanagisawa, S. Koike and K. Yamaji, J. Phys. Soc. Jpn. **67**, 3867 (1998).
- [50] N. F. Mott, *Metal-Insulator Transitions* (Taylor & Francis, London, 1974).
- [51] K. Yosida, *Theory of Magnetism* (Springer, Berlin, 1996).
- [52] T. Misawa and M. Imada, Phys. Rev. B **90**, 115137 (2014).
- [53] T. Yanagisawa, S. Koike and K. Yamaji, J. Phys. Soc. Jpn. **68**, 3608 (1999).
- [54] N. Cancrini, S. Caprara, C. Castellani, C. Di Castro, M. Grilli and R. Raimondi, EPL **14**, 597 (1991).
- [55] S. Caprara, C. Di Castro and M. Grilli, Phys. Rev. B **51**, 9286 (1995).
- [56] J. Lorenzana and G. Seibold, Phys. Rev. Lett. **89**, 136401 (2002).
- [57] F. Günther, G. Seibold and J. Lorenzana, Phys. Rev. Lett. **98**, 176404 (2007).
- [58] L. F. Tocchio, F. Becca and S. Sorella, Phys. Rev. B **94**, 195126 (2016).
- [59] T. Yanagisawa and M. Miyazaki, EPL **107**, 27004 (2014).
- [60] C. Weber, K. Haule, and G. Kotliar, Phys. Rev. B **78**, 134519 (2008).
- [61] M. S. Hybertsen, M. Schluter, and N. E. Christensen, Phys. Rev. B **39**, 9028 (1989).
- [62] H. Eskes, G. A. Sawatzky, and L. F. Feiner, Physica C **160**, 424 (1989).
- [63] A. K. McMahan, J. F. Annett, and R. M. Martin, Phys. Rev. B **42**, 6268 (1990).
- [64] H. Eskes and G. Sawatzky, Phys. Rev. B **43**, 119 (1991).
- [65] H. Otsuka, J. Phys. Soc. Jpn. **61**, 1645 (1992).

- [66] D. Eichenberger and D. Baeriswyl, *Phys. Rev. B* **76**, 180504 (2007).
- [67] D. Baeriswyl, D. Eichenberger and M. Menteshashvili, *J. Phys.* **11**, 075010 (2009).
- [68] D. Baeriswyl, *J. Supercond. Novel Magn.* **24**, 1157 (2011).
- [69] D. Baeriswyl, *Phys. Rev. B* **99**, 235152 (2019).
- [70] T. Yanagisawa, *J. Phys. Conf. Ser.* **1293**, 012027 (2019).
- [71] H. Yokoyama and H. Shiba, *J. Phys. Soc. Jpn.* **56**, 1490 (1986).
- [72] G.-Q. Zheng, Y. Kitaoka, K. Ishida and K. Asayama, *J. Phys. Soc. Jpn.* **64**, 2524 (1995).
- [73] N. Takeshita, A. Yamamoto, A. Iyo and H. Eisaki, *J. Phys. Soc. Jpn.* **82**, 023711 (2013).
- [74] R. Raimondi and C. Castellani, *Phys. Rev. B* **48**, 11453 (R) (1993).